Methyl Dynamics and β-Relaxation in Polyisobutylene: Comparison between Experiment and Molecular Dynamics Simulations

K. Karatasos,*,† J.-P. Ryckaert,† R. Ricciardi,‡ and F. Lauprêtre‡

Department of Physics, Polymer Physics CP-223, Université Libre de Bruxelles, Bd. du Triomphe, 1050 Brussels, Belgium; and Laboratoire de Recherche sur les Polymères, CNRS, 2 à 8 rue Henri Dunant, 94320 Thiais, France

Received July 23, 2001; Revised Manuscript Received October 18, 2001

ABSTRACT: Molecular dynamics simulations were employed in bulk polyisobutylene, to provide a detailed characterization of the methyl dynamics and to examine its relation to the β-relaxation as described by different experimental techniques. The simulation results were compared to new ^{13}C NMR measurements probing methyl motion at temperatures above the glass transition, as well as to lower temperature literature NMR data. It was found that the ^{13}C NMR results, and those for the β-relaxation reported by dielectric relaxation spectroscopy and neutron scattering experiments, can be interpreted on a common basis through a coupling mechanism between methyl rotation and a recently described fast relaxation motion associated with the chain backbone. In addition, a molecular mechanism for the description of the dielectric β-process observed in polyisobutylene is proposed, and investigated by simulations.

I. Introduction

Although polyisobutylene (PIB) is among the most well studied polymers[1−13] due to the technological importance arising from its extraordinary properties,[14] many aspects of its physical behavior are still not well understood. Questions concerning the description of dynamics at short length and time scales associated with local conformational motion (particularly related to the β-relaxation) and methyl rotation, still remain open.

Lately, dielectric relaxation spectroscopy[11] (DRS), neutron spin−echo (NSE)[11] and incoherent quasielastic neutron scattering (IQENS)[10] experiments offered valuable insight on the characteristics of PIB local dynamics. Moreover, they pointed out some intriguing inconsistencies with results from other spectroscopic techniques[1,2] (i.e., NMR), associated mainly with two observations.

(i) The first is the weaker temperature dependence of the temperature shift factors as extracted from NMR experiments, compared to the WLF dependence of the shift factors from the above techniques and from viscosity measurements. Account for this issue was recently provided by molecular dynamics (MD) simulations in the temperature regime where the α- and β-processes merged.[15] The role of a motional mechanism originating from the backbone conformational transitions between the two trans states existing in PIB[5,13] was revealed, and the aforementioned disparity was resolved by examining which piece of information concerning dynamics is accessible to each technique. It was demonstrated that the WLF behavior could be reproduced by the temperature dependence of the overall average relaxation time including contributions from all the different dynamic mechanisms, while NMR measurements, at the particular frequency and temperature range,[4] were shown to selectively probe the slower mechanism of conformational transitions between the trans and gauche states of the chain backbone.

(ii) The second is the apparent inconsistency arising from identification of the so-called δ-relaxation observed in NMR studies at low temperatures, as due to methyl motion.[2] Although the actual relaxation times and the activation energy relevant to the δ-process are in good agreement with the ones ascribed to the β-process probed by DRS, NSE, and IQENS, a "pure" methyl rotation would be dielectrically inactive,[11] while due to symmetry reasons a 3-fold methyl-group jump mechanism would be invisible in coherent scattering. Furthermore, the elastic incoherent scattering factor (EISF), which provides an optimal fit to the data, was found to be compatible with a two-site instead of a three-site jump mechanism expected for methyl rotation. The characteristic jump distance d was estimated to be $d \simeq 2.7$ Å far too large for a methyl reorientation ($d = 1.78$ Å).[16] Therefore, the relation between β-relaxation and methyl rotation, as described by NMR, remains an open question.

In this work, we have extended our previous MD studies,[13,15] and performed new ^{13}C T_1 NMR experiments, to investigate the characteristics of methyl dynamics in PIB and to explore its connection with β-relaxation. The interdependence between methyl and local backbone motions was qualitatively and quantitatively studied by examining the degree of correlation between the associated conformational transitions, while dynamic quantities pertinent to NMR, DRS, and neutron scattering observables were calculated and analyzed in a common framework, providing spatial and temporal characterization of methyl motion.

The paper is organized as follows: in the next section details on the simulated systems are provided, while for validation purposes static quantities are compared to pertinent experimental results. Details on the calculated dynamic functions and the data analysis procedure are given in section III. Results on the dynamics related to methyl motion and comparison to NMR measurements are presented in section IV. In section V, the degree of coupling between methyl motion and fast backbone dynamics and the relevant conformational statistics are explored in the simulated trajectories. The relation

* To whom correspondence should be addressed.
† Université Libre de Bruxelles.
‡ Laboratoire de Recherche sur les Polymères, CNRS.

10.1021/ma011290m CCC: $22.00
Published on Web 01/16/2002

between methyl dynamics and the β-relaxation as observed by the DRS and neutron experiments is discussed in section VI. Finally, a summary of the main findings together with the conclusions of the present study is provided in section VII.

II. Simulation Details and Validation of the Simulation Model

Fully atomistic systems of PIB were generated in the melt state. Each of the systems examined was comprised by five chains of 25 monomer units each. Following the generation of the starting configurations and the initial equilibration by a Monte Carlo procedure (see ref 17 for more detail), the atomistic force field was switched on and 1 or 2 ns (depending on the temperature) of additional equilibration under conditions of constant temperature and pressure (*NPT* ensemble) allowed the system to accommodate the local scale conformational changes due to the introduction of the force field. Details on the force field used for the PIB model can be found in ref 13. Subsequently, production runs of 1−2 ns in the constant energy and volume (*NVE*) ensemble were generated utilizing a time-step of 1 fs, with configurations being stored every 0.5 ps. Following this procedure, trajectories at 300, 346, 388, 446, 496, and 603 K (well above the experimental glass transition temperature) were obtained.

To validate the force field parametrization utilized, the static structure factor and specific volume of the simulated systems were compared with available experimental results. The simulated static structure factor was calculated using the expression

$$S(q) = 1 + \frac{\frac{1}{V}\sum_{\alpha}\sum_{\beta} N_\alpha N_\beta f^\alpha(q) f^\beta(q) \int [g^{\alpha\beta}(r) - 1] e^{iq\cdot r}\, d^3r}{\sum_{\alpha} [f^\alpha(q)]^2} \quad (1)$$

where $g^{\alpha\beta}(r)$ represents the radial distribution function for the pair of groups (α, β). α, β symbolize the different carbon species in the system (α, β = CH_2, CH_3). N_α is the number, and $f^\alpha(q)$ the scattering factors of species α. The scattering factors were calculated through the expressions provided in ref 18. The location of the main intra- (high q) and inter- (low q) molecular peaks are in a good agreement with the experimental X-ray diffraction patterns as shown in Figure 1. Inset a shows $S(q)$ in more detail at the low-q regime from a different experimental work.[11] The more detailed variation of the structure factor is in close agreement with the features characterizing the simulation spectra. Prediction of the specific volume of the simulated systems at the examined temperatures together with the respective experimental measurements[19] are depicted in inset b. The simulation results are in reasonable agreement with the experiment.

III. Analysis Method

Local reorientational motion of backbone and methyl C−H bonds was studied through the second-order autocorrelation function (ACF)

$$G(t) = \frac{1}{2}\langle 3[\hat{h}(t)\cdot\hat{h}(0)]^2 - 1\rangle \quad (2)$$

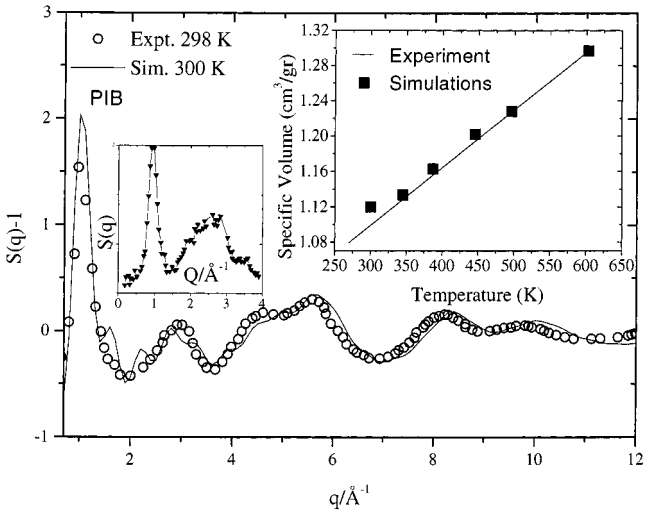

Figure 1. Main panel: comparison of the static structure factor as calculated from simulations (line) and from X-ray scattering experiments (○) by Londono et al.[38] Left inset: static structure factor from a different experimental work.[11] Right inset: comparison of the specific volume of PIB as predicted from the simulated model and as measured experimentally. Error bars on simulation values are of the order of the symbol size at the high temperatures and about twice the symbol size at 300 K and 346 K.[19]

where $\hat{h}$ symbolizes the unit vector along the examined bonds. Spatial and temporal resolution of methylene and methyl hydrogen motion was obtained by calculating the dynamic incoherent structure factor (in the isotropically averaged form)

$$S(q, t) = -\left\langle \sum_{i=1}^{N} \frac{\sin(q\Delta r_i(t))}{q\Delta r_i(t)} \right\rangle \quad (3)$$

In eq 3, N is the number of hydrogen atoms considered, q is the magnitude of the scattering vector, and $\Delta r_i(t) = ||\vec{r}_i(0) - \vec{r}_i(t)||$ is the magnitude of the displacement of the relevant (skeletal or methyl) hydrogen atom. As discussed in previous studies,[5,13,15] apart from the gauche states, the probability distribution for backbone dihedrals in PIB is characterized by the splitting of the trans configuration into two stable states, while the distribution corresponding to methyl dihedrals has the form of a 3-fold potential. Jumps between backbone conformational states will be referred to as t−g and t−t for the transitions between the trans−gauche and the two trans states respectively, whereas methyl jumps will be referred to as m−m.

To treat all the time-dependent spectra in the same way, we have analyzed them by calculating the distribution of relaxation times (DRT)[20,21] corresponding to elementary single-exponential processes according to the expression

$$C(t) = \int_{-\infty}^{+\infty} g(\ln\tau) e^{-t/\tau}\, d(\ln\tau) \quad (4)$$

where $g(\ln\tau)$ symbolizes the normalized (in the logarithmic scale) DRT.[20] It is common to analyze local relaxation data at time and length scales similar to those discussed in the present study, obtained either from experiment[11,22−24] or simulations,[25] by assuming a superposition of single exponential processes. Other commonly used empirical functions employed for analysis of relaxation data, like the stretched-exponential

function, can be described by a superposition of exponentials as well.[26]

In this context, $S(q,t)$ and $G(t)$ functions are described without any a priori assumption regarding the functional form of either the spectra themselves or their corresponding distribution functions $g(\ln \tau)$. Information associated with the existence of distinct motional processes and the dispersion of exponential decays describing each process is extracted from the number and width of the peaks appearing in the DRTs, respectively. A characteristic time (CT) for the i_{th}process appearing in the spectra can be calculated as $\tau_i = \int_{\Delta\tau_i} \tau g(\ln \tau)\, \mathrm{d}(\ln \tau)/\int_{\Delta t_i} g(\ln \tau)\, \mathrm{d}(\ln \tau)$, where $\Delta\tau_i$ denotes the time interval over which the ith peak extends. In the case of symmetric peaks, the location of the maximum provides a good estimate of the CT. If the integration is performed over the entire time window, an average time (including the contribution of all the dynamic processes) τ_{av} is calculated. This estimate of τ_{av} is feasible in our MD experiments when the function reaches zero on the ns time scale of our runs or when it can safely be extrapolated to zero by the DRT analysis. Note also that as the calculated $S(q,t)$ and $G(t)$ functions probe the local dynamics of the chains, an effective ensemble average is made over many independent local processes, so that a reasonable statistical accuracy on these time correlation function up to times of the order of the length of the simulations is effectively observed (for a pragmatic test of this statistical property in the same context of polymer melt local dynamics, see van Zon and de Leeuw[27]).

IV. Methyl Dynamics

A. Methyl Motion As Probed by the Incoherent Dynamic Structure Factor $S(q,t)$. The incoherent dynamic structure factor arising from hydrogen motions can be expressed according to the rotational scattering law[23,28]

$$S_{\text{inc}}(q, \omega) = A_0(q)\, \delta(\omega) + [1 - A_0(q)] \sum_i \frac{1}{\pi} f_i L_i(\omega) \quad (5)$$

where $A_0(q)$ accounts for the elastic incoherent structure factor (EISF) and the second term describes the quasielastic spectra. The $L_i(\omega)$ terms are Lorentzian functions weighted by f_i where $\sum_i f_i = 1$. The EISF for methyl rotation, if a three-site jump model is assumed, is given by[16]

$$A_0(Q) = \frac{1 + 2j_0(Qr_{\text{H-H}})}{3} \quad (6)$$

where j_0 represents the zero-order Bessel function and $r_{\text{H-H}}$ is the hydrogen−hydrogen distance in the CH_3 group.

The time domain expression in its continuous form describing the intermediate scattering function reads as

$$S(q, t) = A_0(q) + [1 - A_0(q)] \int_0^{\infty} f(\tau) \mathrm{e}^{-t/\tau}\, \mathrm{d}\tau$$

$$= A_0(q) + [1 - A_0(q)] \int_{-\infty}^{\infty} g(\ln \tau) \mathrm{e}^{-t/\tau}\, \mathrm{d}(\ln \tau) \quad (7)$$

where $f(\tau) = g(\ln \tau)/\tau$ is the normalized distribution function. In this context the dynamic structure factor is expressed in the general form of eq 4.

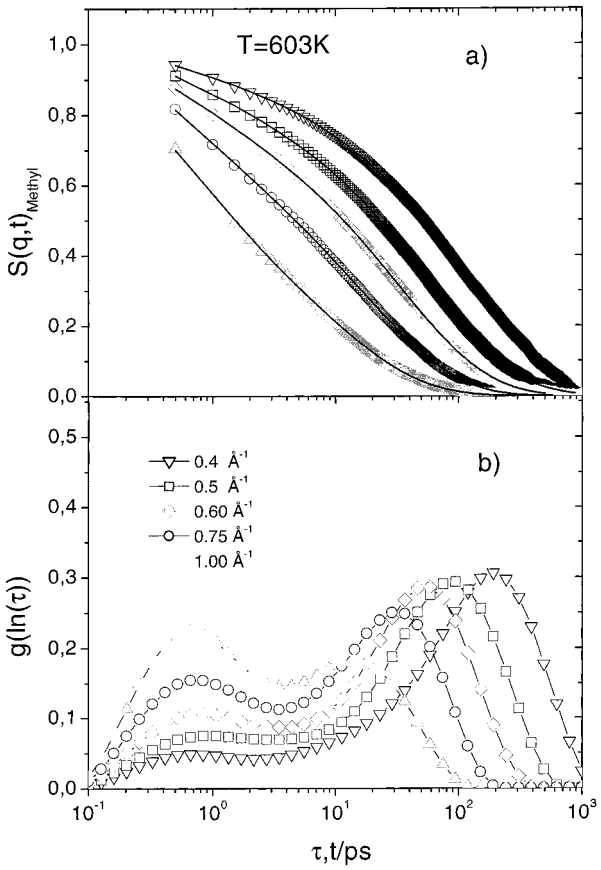

Figure 2. (a) Incoherent dynamic structure factor from the methyl hydrogens at $T = 603$ K for varying scattering vectors $q = 0.4$ Å^{-1}(▽), $q = 0.5$ Å^{-1} (□), $q = 0.60$ Å^{-1}(◇), $q = 0.75$ Å^{-1} (○), and $q = 1.0$ Å^{-1}(△). The lines through the points denote the fits according to eq 4. (b) Corresponding distribution of relaxation times.

Figure 2a shows $S(q,t)$ spectra for the methyl hydrogens at the higher examined temperature at different wave vectors. The lines through the points denote the resulted fits. Corresponding DRTs are plotted in Figure 2b. Apart from the peak at short times reminiscent of the initial decay arising from the fast librational motions[29] (denoted henceforth as FP for fast process), only one process with q-dependent peak location characterizes the distributions in the examined q range. At a lower temperature and at an overlapping q range, this picture changes. In Figure 3 scattering curves and the corresponding DRTs are presented at temperature $T = 496$ K. At the higher q shown, the distribution is bimodal consisting of the FP and one rather broad process. At lower scattering vectors however, the broad peak appears to split into an intermediate process, with an apparently q-independent peak location, and a slower one whose peak location depends on the scattering vector. At an even lower temperature, as shown in Figure 4, aside from the FP at short times, the double featured distributions persist to the higher q examined. At wave vectors higher than the ones shown, analysis was not carried out, since the rapid initial decay of the scattering curve combined with the lack of time-resolution, would lead to a poor fitting.

Focusing on the temporal and spatial features of the observed processes at the lower temperatures (only dynamics slower than FP will be discussed from now on) the following characteristics must be noted: (i) the apparent insensitivity of the location of the maximum

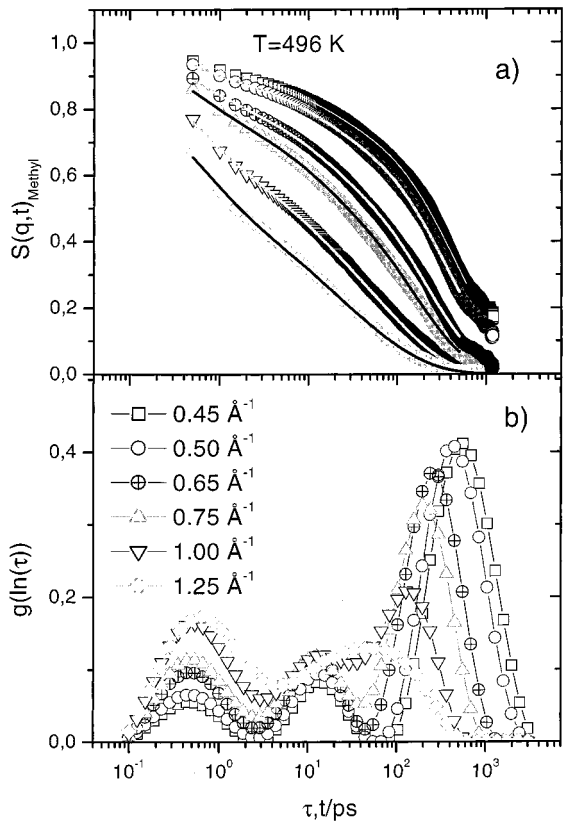

Figure 3. (a) Incoherent dynamic structure factor from the methyl hydrogens at $T = 496$ K for varying scattering vectors $q = 0.45$ Å^{-1} (□), $q = 0.5$ Å^{-1} (○), $q = 0.65$ Å^{-1}(⊕), $q = 0.75$ Å^{-1} (△), $q = 1.0$ Å^{-1}(▽). and $q = 1.25$ Å^{-1} (◊). The lines through the points denote the fits according to eq 4. (b) Corresponding distribution of relaxation times.

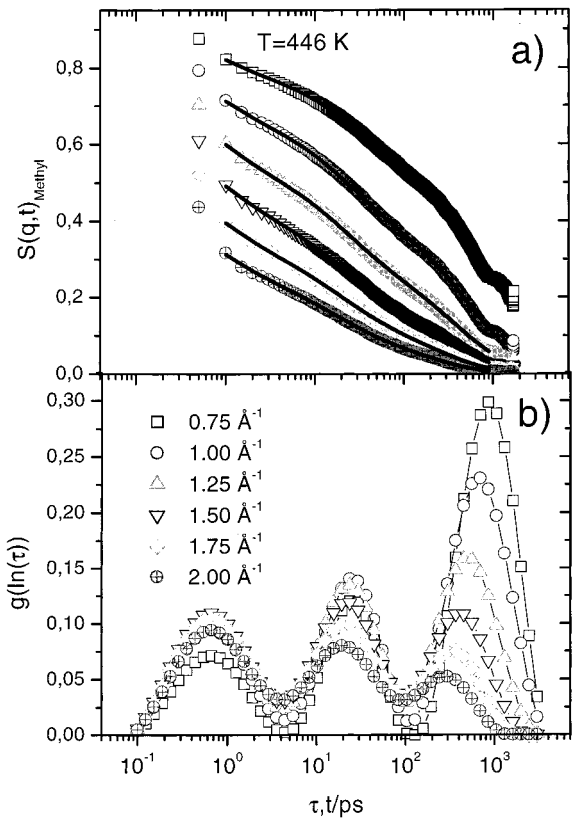

Figure 4. (a) Incoherent dynamic structure factor from the methyl hydrogens at $T = 446$ K for varying scattering vectors $q = 0.75$ Å^{-1} (□), $q = 1.0$ Å^{-1} (○), $q = 1.25$ Å^{-1} (△), $q = 1.50$ Å^{-1}(▽), $q = 1.75$ Å^{-1} (◊). and $q = 2.0$ Å^{-1} (⊕). The lines through the points denote the fits according to eq 4. (b) Corresponding distribution of relaxation times.

of the intermediate process (i.e., its characteristic time) with respect to q, in contrast to the q-dependent peak position of the slower process; (ii) the weaker temperature-dependence exhibited by the intermediate process, when compared to the temperature dependence of the slower process at a constant q. For instance, at $q = 0.75$ Å^{-1}, the characteristic time of the intermediate process slows down by approximately a factor of 2 when the temperature is decreased from 496 (Figure 3b) to 446 K (Figure 4b), while the corresponding factor for the slower process is about 5. Extrapolation of this behavior to higher temperatures, would suggest that these processes merge, as is actually observed at $T = 603$ K.

The above-described features bear a close analogy to the behavior exhibited when backbone hydrogens are probed.[15] To illustrate this analogy, we compare the dynamic structure factor (insets) and the corresponding DRTs of backbone and methyl hydrogens, at different temperatures, and at suitable scattering vectors so that the two processes are separated. At all temperatures as shown in Figure 5a−c, the intermediate process of the methyl spectra appears slower compared to the intermediate peak of the backbone, whereas the slower process of the methyl is somewhat faster than its backbone analogue. The two relaxations characterizing the backbone spectra in this temperature range, were attributed[15] to the t−t (intermediate) and the t−g (slower) conformational mechanisms. The fact that the methyl group is directly attached to the main chain, combined with the fact that at this temperature range (about 200 K above the glass transition temperature) the chain backbone is considerably mobile, can account for the appearance of a backbone-related slow mode in the methyl spectra. The intermediate process appearing in the methyl−hydrogen scattering spectra, should inevitably be associated with a mechanism that involves methyl rotation. Its fast time scale, close to the independently calculated inverse m−m transition rates,[13] its q-independent character, and its weaker temperature dependence support this assignment.

On these grounds, we can examine if a model that is commonly employed to describe methyl motion in polymer glasses,[23] is able to provide a reasonable description for this process. In previous studies, methyl rotation or other local motions such as the β-relaxation were modeled assuming a log−Gaussian form for the associated distribution of relaxation times or, equivalently, a Gaussian distribution of barrier heights hindering the motion.[10,23,28] This approach was also successfully applied at temperatures well above the glass transition, since for a given polymer there are strong indications that the distribution of potential barriers is not very sensitive to the glass transition.[30] In this context, the DRT is expressed as

$$g(\ln \tau) = \frac{RT}{\sigma \sqrt{\pi}} \exp\left[-\frac{RT \ln(\tau/\tau_0) - E_0}{\sigma}\right]^2 \qquad (8)$$

This expression is derived by assuming that in the energy domain, the examined process can be represented by a Gaussian distribution of activation energies $g(E) = 1/\sigma \sqrt{\pi} \exp[-(E - E_0/\sigma)^2]$, and that the characteristic time τ follows an Arrhenius temperature depen-

Table 1. Fitting Parameters from Eq 8

T/K	E_0 (kJ/mol)	σ (kJ/mol)
388	25.97 ± 0.03	4.39 ± 0.06
446	26.26 ± 0.03	4.19 ± 0.05
496	26.93 ± 0.05	3.62 ± 0.07

dence with activation energy E, namely $\tau(T) = \tau_0 \exp(E/RT)$. E_0 represents the average activation energy, σ the width of the distribution of the barrier heights, and τ_0 the inverse of an attempt jump frequency. In our case, τ_0 was fixed to the value $\tau_0 = 0.019$ ps obtained from the description of methyl rotation in polyisoprene (PI), where the CH_3 group is directly attached to the chain as in PIB.[30] The resulting fits are represented by solid lines in the main panel of Figure 5a−c. Apparently, the log−Gaussian model provides a satisfactory fit to the distribution of the intermediate process. The average barrier heights and the corresponding widths extracted from these fits are listed in Table 1.

The widths of the distribution are moderately temperature dependent and comparable to those reported for PI, $\sigma = 4.38$ kJ/mol[31] and $\sigma = 5.02$ kJ/mol,[30] and for atactic polypropylene (aPP),[32] $\sigma = 4.95$ kJ/mol (note that in our definition a factor of $\sqrt{2}$ is included in σ). The average barrier height shows a weak dependency on temperature and appears significantly larger (by almost a factor of 2) than in PI or in aPP. In addition, the geometry of the motion corresponding to the intermediate process shown in Figure 5, has not been found to conform to that of an independent methyl rotation. CH_3 group rotation in PI or in other polymers[28] as probed by neutron scattering experiments, or as observed in simulation studies,[33] is generally found to be satisfactorily described by a jump process between three equivalent sites, exhibiting the corresponding EISF (eq 6). In PIB, the EISF associated to the intermediate process of the methyl spectra, as calculated by the corresponding amplitude, could not be fitted with such a model. A possible reason underlying this failure is already indicated in Figures 5a−c. As shown, there is a significant overlap in the time scales between the intermediate process in methyl spectra and the t−t mechanism contributing to the backbone motion. The characteristic time of the t−t mechanism is shorter than the characteristic time of methyl motion as inferred from the locations of the corresponding peaks, and the respective transition rates.[15,13] Therefore, the methyl-hydrogen displacement in this time scale may well be affected by such a rapid backbone rearrangement, so that what is actually probed by scattering techniques is a modified process differing from a "pure" methyl rotation. This picture is consistent with the fact that, when the mean square displacement of methyl-hydrogen atoms between m−m jumps from the simulation is calculated (the time is set to 0 at any methyl jump and stops at the next jump of the same methyl), it is found significantly larger than the distance of 1.78 Å corresponding to the geometry of a "pure" methyl rotation. For instance at $T = 346$ K the mean square displacement was $\sqrt{\langle \Delta r^2 \rangle} = 2.6$ Å. As the t−t mechanism assumes a low activation energy (≃11 kJ/mol),[15] it is expected to remain active at very low temperatures, affecting therefore the methyl motion even in the sub-T_g regime.

An informative check of the analysis of simulated $S(q,t)$ functions discussed in this section would ideally come from incoherent neutron data on partially deuterated PIB material, but so far such data are not available. We will come back on neutron scattering data on fully hydrogenated samples in a later section devoted to the β-relaxation in PIB.

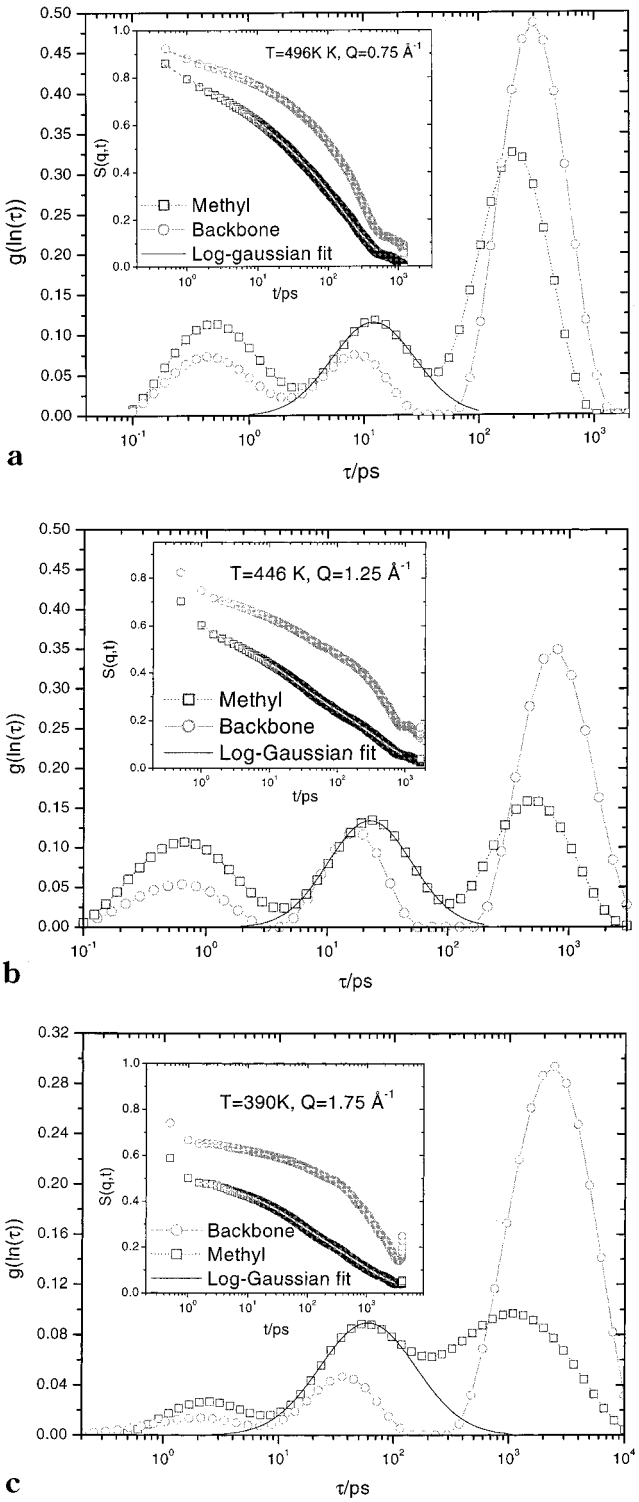

Figure 5. Main panel: comparison of DRTs from $S(q,t)$ data from the methyl (□) and methylene (○) hydrogens. The continuous line represents the fit of the intermediate process according to expression 8. The inset shows the actual spectra (symbols) together with the corresponding fits (lines): (a) $T = 496$ K, $q = 0.75$ Å^{-1}; (b) $T = 446$ K, $q = 1.25$ Å^{-1}; (c) $T = 388$ K, $q = 1.75$ Å^{-1}.

B. Reorientational Dynamics of Methyl Motion As Probed by $G(t)$. Figure 6a shows the $G(t)$ ACFs at different temperatures. Lines through the points denote

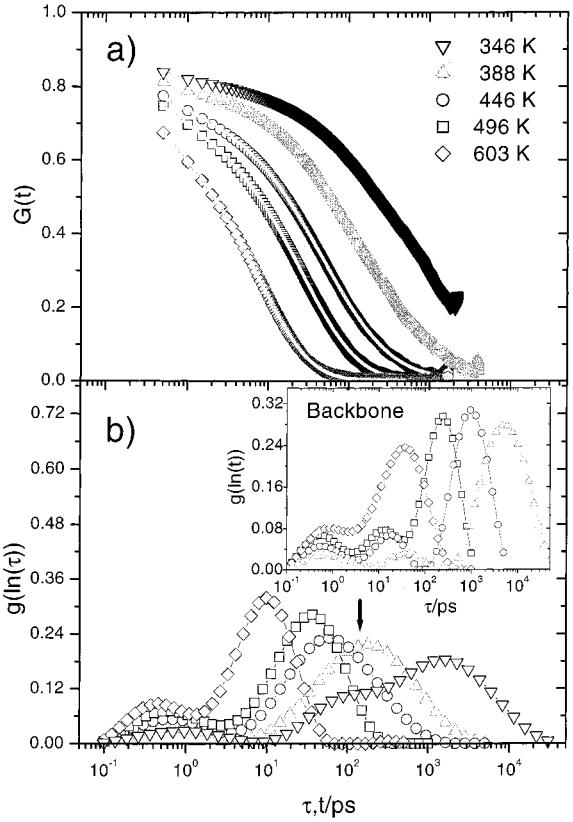

Figure 6. (a) Second-order orientational correlation function of methyl C−H bonds, at temperatures $T = 346$ K (▽), $T = 388$ K (△), $T = 446$ K (○), $T = 496$ K (□), and $T = 603$ K (◇). The lines through the points represent the resulting fits. (b) Main panel: Corresponding distribution of relaxation times. Inset: distributions of relaxation times corresponding to spectra from backbone C−H bonds at the same temperatures. The vertical arrow denotes the peak location of the intermediate process appearing in the $S(q,t)$ spectra (not shown here) at $T = 346$ K.

the fit calculated according to eq 4. The corresponding DRTs are presented in Figure 6b. The distributions describing backbone motion are shown for comparison in the inset. The assignment of the peaks characterizing the backbone distribution spectra is the same as that for the dynamic structure factor of the methylene hydrogens.[15] The first process is ascribed to the FP, and the intermediate peak is assigned to the t−t mechanism, while the slower process at the examined temperature range follows the t−g dynamics. However methyl motion, as probed by the reorientation of the C−H bond, seems to probe a local environment described by a broader dispersion of characteristic times: apart from the temperature-independent peak located at very fast time scales, a single relaxation process describes the distributions at temperatures $T \geq 388$ K. This process is progressively broadened and shifted to lower times as temperature decreases. It is worthwhile to note that its time span overlaps with both the intermediate and the slow peak of the backbone motion at $T < 603$ K. At the lowest temperature shown ($T = 346$ K), there is an indication for a splitting of the broad peak. The time scale of the "shoulder" developed in the distribution at the short time side compares favorably to the location of the maximum of the q-independent peak appearing in the corresponding $S(q,t)$ curves (not shown here) as indicated by the arrow in Figure 6b. The splitting of the broad process at low temperatures is consistent with

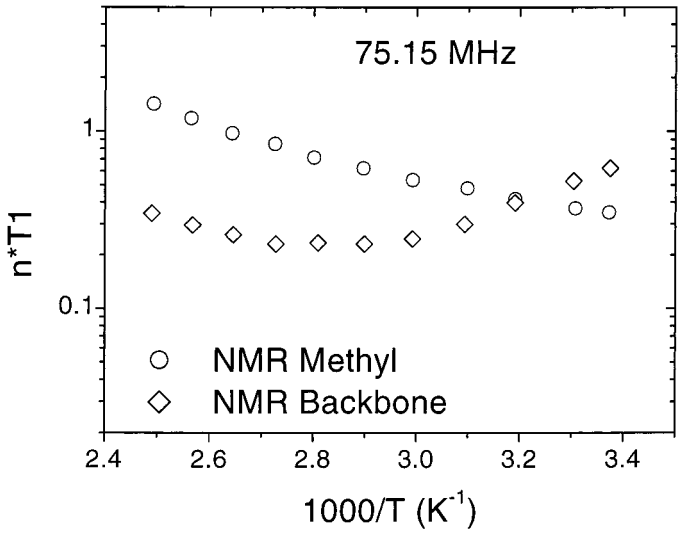

Figure 7. T_1 NMR measurements for backbone (◇) and for methyl (○) motion at 75.15 MHz.

the existence of two underlying processes with distinct temperature dependencies as observed in the $S(q,t)$ spectra.

To obtain experimentally specific indications on methyl reorientation dynamics, new ^{13}C T_1 NMR measurements have been conducted in the temperature range 300 K < T < 400 K. These measurements probe $G(t)$ through its spectral density

$$J(\omega) = \frac{1}{2}\int_{-\infty}^{\infty} G(t)e^{i\omega t}\,dt \qquad (9)$$

Spin−lattice ^{13}C NMR measurements are then described as

$$\frac{1}{T_1} = Kn[J(\omega_H - \omega_C) + 3J(\omega_C) + 6J(\omega_H + \omega_C)] \qquad (10)$$

where ω_H and ω_C are the resonance frequencies of ^1H and ^{13}C, while K is a constant associated with their gyromagnetic ratios[4] and n is the number of bonded protons. T_1 NMR measurements for PIB methyl carbons are shown in Figure 7 at 75.15 MHz. Corresponding data for the backbone carbons are shown as well for comparison. Data represented in Figure 7 clearly show that the T_1 values obtained for the CH_2 and the CH_3 carbons as a function of temperature are not proportional, and that the temperatures at which the T_1 minimum is observed for these two kinds of carbons, are different. These results indicate that the methyl group does not relax via the chain motion only, but also via its internal rotation. Backbone C−H reorientation for polymers far above T_g is usually well described by the DLM functional form[4] in terms of a damped diffusion of bond reorientations and independent librations. For fast librations, $G(t)$ is expressed as

$$G(t) = (1 - \alpha)e^{-t/\tau_1}e^{-t/\tau_2}I_0(t/\tau_1) \qquad (11)$$

where I_0 is the modified Bessel function of order 0, τ_1 is the characteristic time for the diffusion of the C−H bond orientation, τ_2 is the damping term, and α is related to the half-angle θ of the libration cone through the expression

$$1 - \alpha = \left[\frac{\cos\theta - \cos^3\theta}{2(1 - \cos\theta)}\right]^2 \tag{12}$$

Analysis of the NMR data for the backbone C−H bonds in PIB[15] led to a main-chain segmental time τ_1 presenting a slower temperature dependence with respect to the rheological WLF relaxation time. As discussed in the Introduction, this τ_1 relaxation time was shown to be related to the "slow" backbone dynamics associated with t−g jumps which occur in the time window of the NMR experiment.

The interpretation of the methyl C−H bond reorientation in the examined temperature range is clearly more complex, as implied from the $S(q,t)$ and $G(t)$ analysis of the simulation data: the dynamics reflects methyl rotation that is affected by the backbone relaxation. These motions appear to contribute to a broad peak of the DRT function of $G(t)$ at high temperatures, but seem to become distinct as T is lowered.

The latter trend at low T suggests to interpret methyl NMR data with a simplified functional form

$$G(t) = G(t)_{\text{Back.}} * G(t)_{\text{rot.}} \tag{13}$$

where $G(t)_{\text{Back.}}$ corresponds to the backbone related motion and $G(t)_{\text{rot.}}$ represents a decoupled methyl rotation. Such a description assumes independent processes for backbone and methyl dynamics both being accessible within the experimental time window. For this model (to which we will refer as model A) a natural choice is to retain the DLM functional form for the backbone contribution $G(t)_{\text{Back.}}$ with the correlation times τ_1 and τ_2 determined from the chain CH_2 carbons, while for $G(t)_{\text{rot.}}$, a functional form describing the C−H bond motion in a CH_3 group undergoing intramolecular reorientation about its symmetry axis[34] can be adopted

$$G(t)_{\text{rot.}} = A + Be^{-t/\tau_3} + Ce^{-4t/\tau_3} \tag{14}$$

$$A = \frac{(3\cos^2\psi - 1)^2}{4}$$

$$B = \frac{3\sin^2 2\psi}{4}$$

$$C = \frac{3\sin^4\psi}{4}$$

where ψ is the angle between the methyl C−H bond and the C−CH_3 axis and τ_3 is the correlation time of the methyl group motion.

Alternatively, prompted by the existence of a single broad process (apart from the uninteresting FP) in the $G(t)$ distributions at $T > 346$ K, and the similarity in the temperature dependence of backbone and methyl T_1 measurements at high temperatures (see Figure 7), we can attempt to describe the methyl NMR data as a single "effective" process where methyl rotation and backbone contributions are mixed. A way to represent such an "effective" process is by describing it through the DLM function with correlation times τ_1' and τ_2'

$$G(t) \propto G'_{\text{DLM}}(t) \tag{15}$$

This approach will be referred to as model B.

The ratio τ_2'/τ_1' was fixed to a value of 40 as obtained from the chain carbons,[4] while α was estimated to be 0.72 for model A and 0.36 for model B.

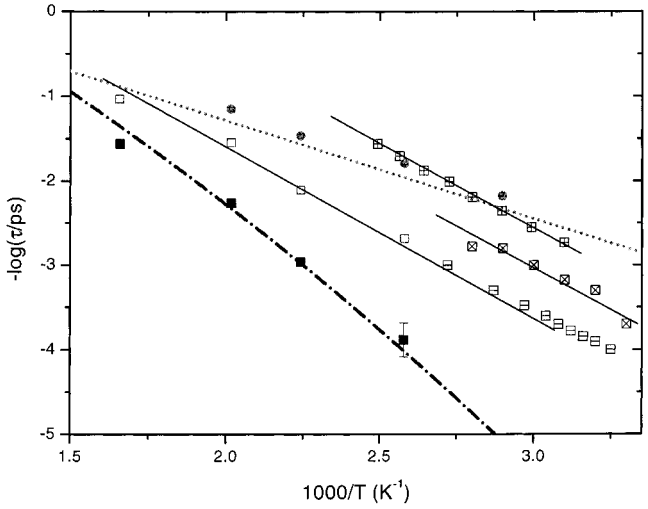

Figure 8. Activation plot displaying the comparison of low- and high-temperature NMR relaxation times to simulation results. Average relaxation times (τ_{av}) corresponding to backbone C−H motion (■) together with the experimental WLF behavior for the α-relaxation (dash−dotted line) are shown for comparison as well. The extrapolation of low-temperature NMR data (dotted line, ref 1) is compared to the temperature behavior of the q-independent times corresponding to the intermediate process appearing at the $S(q,t)$ spectra (●) described in section IVA. The temperature dependence of the average times (□) describing the slow process of the methyl C−H simulation spectra (Figure 6b, main panel), is compared to the common Arrhenius behavior (solid line through the points) followed by the NMR relaxation times calculated as described in the text (open square with horizontal bar for τ_1, open square with × for τ_3, and ⊞ for τ_1').

Comparison between the times extracted from fitting the NMR data by the two models, and the average time (□) corresponding to the main broad process of the simulation methyl $G(t)$ curves, is shown in Figure 8. τ_1 (open square with horizontal bar) and τ_3 (open square with ×) as obtained from model A exhibit a similar temperature dependence, implying an interrelation between methyl rotation and backbone motion, which seems to subside the hypothesis of a simple decoupled model as represented by eq 13. Apart from the noted difference in absolute time scales, analysis of the new NMR data on methyl dynamics leads to a well-defined temperature dependence of the main relaxation time (as calculated either from model A or from model B (τ_1', ⊞)), which agrees with the DRT analysis of simulation data (□), but is unable to disentangle the methyl and backbone individual motions which appear to be mixed in a subtle way.

To relate results from the simulation to low-temperature literature NMR data, it is interesting to combine information from $G(t)$ and $S(q,t)$ functions relevant to methyl dynamics. As mentioned earlier, the intermediate process resolved in $S(q,t)$ (Figure 3 and 4), which in a certain q range is distinct from the slow backbone conformational motion, is also observed in methyl $G(t)$ curves upon decrease of the temperature, as indicated by the $T = 346$ K DRT (Figure 6b). On the basis of the $S(q,t)$ behavior, if we assume that the two processes characterizing $G(t)$ at $T = 346$ K will be further separated in time scale as the temperature decreases, it follows that the sub-T_g NMR experiments will selectively probe the fastest of the two modes since, at these temperatures, it will be in the accessible frequency range while the slower process will be much too slow to

be observed. Pursuing this scenario, we have compared the extrapolated low-temperature NMR behavior assigned to methyl motion[1] (dotted line) to the behavior of the *q*-independent intermediate process resolved in $S(q,t)$ of methyl hydrogens (●) as depicted in Figure 8. Apparently, there is a close agreement between the two data sets, lending support to the assignment of the intermediate process observed in the methyl hydrogen $S(q,t)$ as due to methyl motion.

On the probed time scales, this methyl motion appears to be definitely more complex than what is predicted by simple three-site jump model resulting from the rotation of the methyl group around a fixed axis. This is suggested by our present analysis of the methyl NMR data, the reorientation of the methyl C−H bonds (simulated $G(t)$), and also by the analysis of the simulated intermediate incoherent scattering function of the methyl hydrogen atoms, where the associated EISF could not be fitted with the classical three-site jump model. Moreover, in the last case, independent calculations of the mean jump length in space of methyl hydrogen between methyl jumps were found to involve too large values for such a simple model. As a possible origin for this intriguing behavior, we propose the coupling between methyl rotation with the fast backbone t−t mechanism. Driven by the indications for the existence and for the potential importance of such a coupling mechanism for the characterization of methyl motion in PIB, we have studied its extent by monitoring correlated t−t jumps and m−m transitions (representing methyl rotation) as a function of temperature.

V. Correlated Transitions

The idea of a possible coupling between motion of α-methyl groups (attached directly to the main chain) to backbone motion has already been considered in early experimental studies. Authors in refs 34 and 35, prompted by the observation that the T_1 minimum ascribed to CH_3 rotation of PIB occurs at a temperature close to the temperature of the minimum corresponding to motion of the main chain, suggested that some kind of backbone movement is involved in the release of the methyls from hindrance to rotation.

The correlation mechanism between conformational transitions was studied by estimating the number of jumps of the *coupled* species, following a transition of the *triggering* species. The time was set to 0 at the triggering event, and the number of transitions per time unit of the coupled species was monitored as a function of the time lapsed after the triggering transition. The methyl jumps were considered as the triggering species and the t−t transitions as the coupled species. The backbone dihedrals with central bonds containing the carbon to which the methyl of the triggering dihedral is attached, are termed as *first neighbors* (ϕ_2, ϕ_3 in the schematical representation shown in Figure 10). In a similar way *second* (ϕ_1, ϕ_4 in Figure 10) or higher order neighbors on the chain backbone, can be defined. Figure 9 depicts the (ensemble and time) average of the t−t jumps per triggering methyl jump and per time unit (ps) of the first two neighbors, as a function of time after the triggering event, for the three higher temperatures. The *y*-axis is normalized to the uncorrelated average of the t−t transitions at each temperature. This probability is symmetric in time, so that its decay at positive time is equivalent to a built up of probability at negative (prior to the triggering event) time.

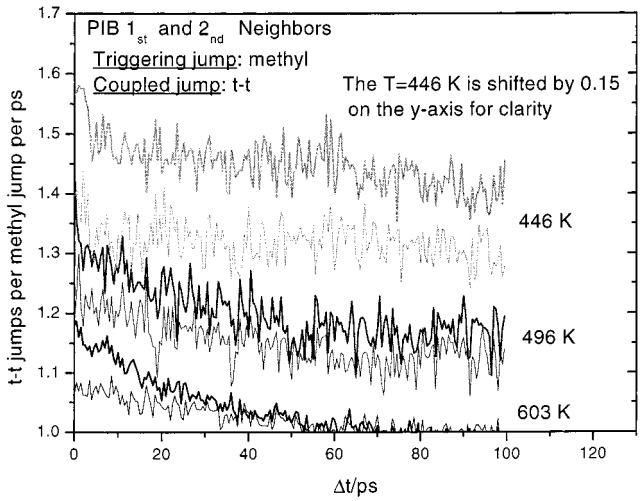

Figure 9. Coupling between the t−t and the m−m transitions (see text) at three temperatures. Thick lines correspond to first neighbors and thin lines to second neighbors. The $T = 446$ K results are translated by a factor of 0.15 in the *y*-axis for clarity.

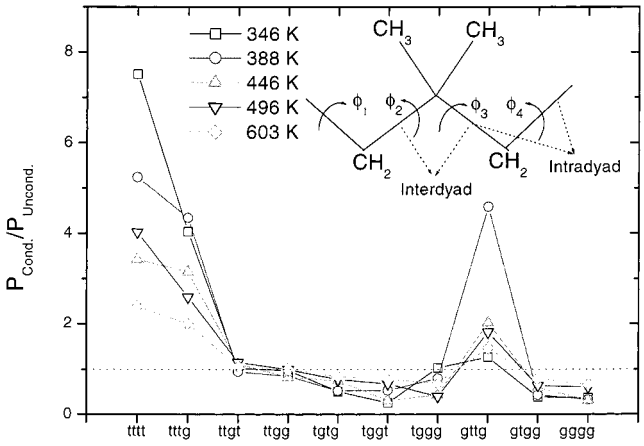

Figure 10. Ratio of the probability of observing a 4 backbone dihedral sequence when a m−m jump takes place, over the unconditional probability of the appearance of each specific conformational sequence. The inset shows the definition of an intradyad and an interdyad in PIB.

At the highest temperature studied, only a moderate excess probability is observed at times close to the triggering transition, which however is rather long-lived, reaching the background value after almost 60 ps. At lower temperatures, although the statistics are worse (since both kinds of transitions become more rare), the trend of the enhancement of coupling, as well as its longevity in comparison to the higher temperature behavior, is beyond the error. Therefore, the coupling between the backbone t−t transitions and the methyl rotation is expected to persist and to be significant at lower temperatures. A similar study of coupling between methyl jumps revealed an enhanced probability of co-rotation of the methyls which are attached to the same carbon. Such a concerted motion of the two methyl groups is consistent with the observation that the average barrier height for methyl motion in PIB is almost twice as much compared to the one for polymers possessing a single methyl side group, like PI or aPP as mentioned earlier.

To check which backbone conformations facilitate methyl motion and promote the observed coupling, we have calculated the probability of appearance of the

Table 2. Conditional and Unconditional Probabilities of 4-Dihedral Sequences Including the Two Intradyads

T/K	346	388	446	496	603
tttt	0.139(0.018)	0.182(0.035)	0.087(0.025)	0.073(0.018)	0.046(0.019)
tttg	0.171(0.042)	0.152(0.035)	0.139(0.044)	0.105(0.040)	0.105(0.052)
ttgt	0.277(0.273)	0.260(0.275)	0.284(0.253)	0.259(0.224)	0.237(0.223)
ttgg	0.150(0.154)	0.119(0.140)	0.089(0.107)	0.139(0.139)	0.151(0.151)
tgtg	0.090(0.176)	0.097(0.187)	0.191(0.256)	0.221(0.285)	0.023(0.033)
tggt	0.003(0.011)	0.008(0.015)	0.004(0.013)	0.009(0.014)	0.219(0.262)
tggg	0.059(0.057)	0.027(0.034)	0.015(0.035)	0.015(0.038)	0.017(0.022)
gttg	0.010(0.008)	0.039(0.008)	0.051(0.025)	0.039(0.022)	0.038(0.026)
gtgg	0.096(0.248)	0.109(0.252)	0.137(0.232)	0.133(0.209)	0.156(0.199)
gggg	0.005(0.013)	0.006(0.018)	0.003(0.008)	0.006(0.010)	0.007(0.011)

conformational states including the first and second neighbors of the rotating methyl group (sequences of four backbone dihedral angles) as schematically depicted in the inset of Figure 10. Any such conformational sequence is represented as $\phi_1\phi_2\phi_3\phi_4$ where ϕ_1, ϕ_2, ϕ_3, ϕ_4 can be either trans (t) or gauche (g) (no distinction between t^+ and t^- or g^+ and g^- is made). This probability was calculated under the condition that one of the methyl groups attached to the carbon located at the middle of the sequence undergoes a transition. Table 2 lists the calculated values, together with the respective unconditional probabilities given in parentheses for comparison purposes. Probabilities for mirror image quadruplets have been summed up. Inspecting the unconditional probabilities, it becomes apparent that at all temperatures the most probable sequences are those of the $\phi_1$tgϕ_4 type, where ϕ_1 and ϕ_4 are t or g. This occurrence is consistent with previous results obtained by conformational energy calculations of PIB.[35,3] In the conditional probabilities, it is remarkable that conformations of the $\phi_1$ttϕ_4 type are significantly enhanced, assuming higher values at lower temperatures. On the other hand, the conditional probabilities for the conformational sequences of the $\phi_1$ggϕ_4 and certain of the $\phi_1$tgϕ_4 types (i.e., tgtg and gtgg) are reduced. A visual impression of these effects is provided in the main panel of Figure 10, where the ratio of the conditional over the unconditional probabilities for all the conformational types and for all the examined temperatures is plotted.

The increase of the conditional probability for the $\phi_1$ttϕ_4 type at the expense of $\phi_1$tgϕ_4 or $\phi_1$ggϕ_4 conformations compared to the unconditional case should therefore be related to the excess correlation between the methyl and the t−t jumps depicted in Figure 9. In other words, the coupling between methyl and backbone motion could be viewed as an indirect consequence of the fact that the tt *interdyad* conformations promote an enhancement of the probability of both the t−t jumps and the methyl transitions. In this context, since t−t transitions occur on a faster time scale than methyl jumps, the displacement of the hydrogen atoms involved in a methyl rotation is expected to be augmented due to the t−t conformational jumps, in accordance with results described in section IVA.

VI. Methyl Motion and β-Relaxation in PIB

A. Connection with the Dielectric β-Relaxation. In order for a local (or global) polymer relaxation mechanism to be dielectrically active, a permanent dipole moment of sufficient magnitude pertinent to this motion, must be present. In frequency domain DRS, the complex dielectric permittivity $\epsilon^*(\omega)$ is probed as a function of the frequency of the applied electric field. This quantity is associated with the one-sided Fourier transform of the underlying correlation function $\Phi(t)$ through the relation

$$C(\omega) = \frac{\epsilon^*(\omega) - \epsilon_\infty}{\epsilon_0 - \epsilon_\infty} = \int_0^\infty \left[-\frac{\mathrm{d}\Phi(t)}{\mathrm{d}t}\right] \mathrm{e}^{-i\omega t}\, \mathrm{d}t \quad (16)$$

where ϵ_0 and ϵ_∞ are the dielectric constants in the limit of 0 and infinite frequency, respectively. $\Phi(t)$ represents the first order dipole autocorrelation function (cross correlation terms are usually very small and can be omitted in a first approximation)

$$\Phi(t) = \frac{\langle \hat{\mu}(0)\hat{\mu}(t)\rangle}{\langle \mu(0)^2\rangle} \quad (17)$$

where $\hat{\mu}$ is the vector along the dipole moment. Due to the absence of strong polar groups and the symmetry of its microstructure, PIB would be a very poor candidate for dielectric experiments. Nevertheless, dielectric measurements have been reported in the past,[14] but the dielectric signal was surmised to emerge from defects of the microstructure or from partial oxidation of the material. Recently, DRS measurements with a high-resolution apparatus were reported for PIB.[11] Although probability of oxidation was not excluded, detection of a very low signal arising from a small intrinsic dipole moment was considered possible.

If the dielectrically observed β-relaxation arises from a dipole moment related to the backbone, it follows that the similarity in temperature dependence among the two motions (methyl and β-process), can be justified through the coupling mechanism between backbone and methyl motion as described in the previous sections. From another point of view, taking into account the microstructure of PIB, it appears plausible that a net dipole moment (although weak) can be related to the methyl group. Due to the symmetry of the CH_3 group, a simple methyl rotation would not change the reorientation of the dipole, rendering this motion invisible to DRS. However, a correlated motion arising from the *combination* of the two methyl groups attached to the same carbon, which could be equivalently described by reorientation of a resultant dipole moment, may be dielectrically active. Such a motion could be facilitated to a lesser extent by the relative reorientation of the two $C-CH_3$ bonds and to a larger extent by backbone motion which would involve the concurrent movement of the two CH_3 groups. To explore the dynamic features of such a combined motion, we investigated the orientational relaxation of a vector which lies on the direction of the bisector of the CH_3-C-CH_3 angle as is schematically shown in the lower panel of Figure 11.

It should be noted that the analysis of a correlation function representing dipole reorientation can be per-

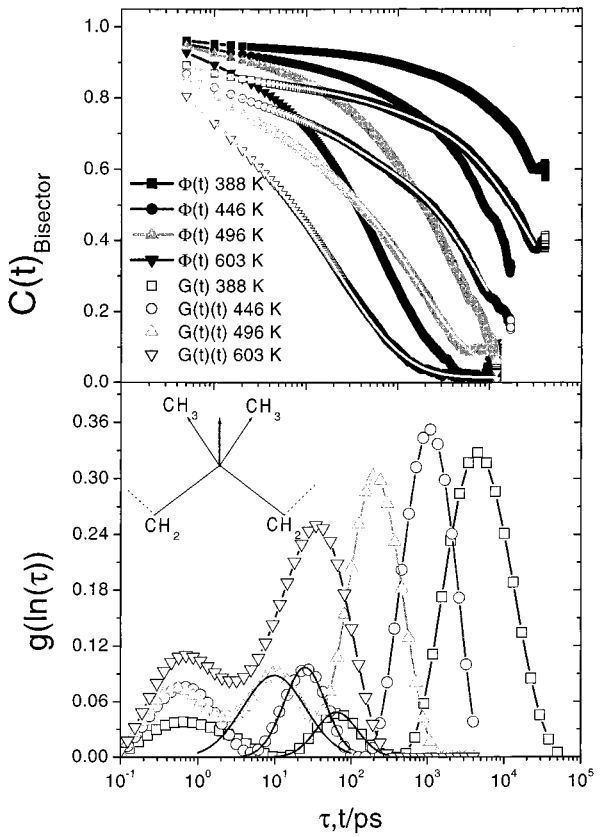

Figure 11. (a) First-order ($\Phi(t)$, solid symbols) and second-order ($G(t)$, open symbols) orientational correlation functions for the bisector vector at temperatures $T = 388$ K (□), $T = 446$ K (○), $T = 496$ K (△), and $T = 603$ K (▽). The lines through the $G(t)$ curves denote the resulted fits. (b) Schematical representation of the vector lying on the bisector of the two $C-CH_3$ bonds, together with the distribution of relaxation times corresponding to the $G(t)$ spectra. The solid lines represent the fit to the intermediate process according to eq 8.

formed in the context of eq 4. It is common to express $C(\omega)$ (eq 16) as a superposition of Debye functions[11,36]

$$C(\omega) = \int_{-\infty}^{+\infty} g(\ln \tau) \frac{1}{1 + i\omega\tau} \, \mathrm{d}(\ln \tau) \qquad (18)$$

which is equivalent to describing $\Phi(t)$ by a superposition of exponentials. To compare DRS results to methyl and backbone motions discussed earlier, both first-order (eq 17) and second-order (eq 2) autocorrelation functions of the bisector vector were calculated. Figure 11a shows the first- ($\Phi(t)$) and second-order ($G(t)$) correlation functions at different temperatures. The lines through the $G(t)$ curves correspond to the DRTs appearing in Figure 11b. DRTs are shown for $G(t)$ data only, due to their higher degree of decorrelation as compared to $\Phi(t)$ curves within the simulation window. Except for the ultrafast process analogous to the FP, an intermediate and a slower process are clearly resolved in the distributions, bearing strong similarity to the behavior of backbone motion (see inset in Figure 6b). An attempt to fit the intermediate process with a log−Gaussian form (eq 8) which provided a good description of the dielectric β-relaxation spectra,[11] yielded average activation barriers of 26.24 ± 0.04 kJ/mol at $T = 388$ K, 26.60 ± 0.06 kJ/mol at $T = 446$ K and 25.69 ± 0.1 kJ/mol at $T = 496$ K. τ_0 was kept at the same value as in the case of the methyl process (sec. IVA). These estimates compare well to the value of $E_0 = 25.1$ kJ/mol found for

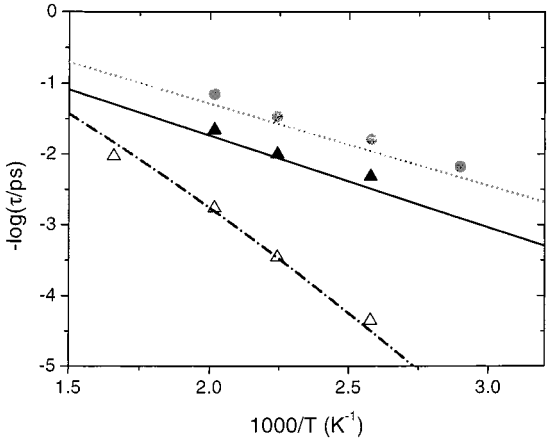

Figure 12. Activation plot showing the comparison between the high-temperature extrapolation (solid line) of the dielectric β-relaxation,[10] to the times corresponding to the intermediate process of the $\Phi(t)$ spectra (▲) calculated from the $G(t)$ analogues as described in the text. The associated overall (including thus all the processes shown in Figure 11b) average times (△), are compared to the WLF behavior of the dielectric α-relaxation.[10] In addition, the extrapolation of low-temperature NMR data (dotted line) together with the q-independent times corresponding to the intermediate process appearing at the $S(q,t)$ spectra (●) are repeated from Figure 8, for a direct comparison.

the dielectric β-process,[11] as well as to the values corresponding to the methyl process resolved in $S(q,t)$ (Table 1).

Figure 12 compares the average times corresponding to the intermediate process as calculated from $G(t)$ spectra, to the extrapolated times of the lower temperature dielectric data for the β-relaxation.[10] Together, the extrapolation of the low-temperature methyl NMR data and times of the methyl process as calculated from simulations (taken from Figure 8), as well as the overall average $G(t)$ times, are also plotted. The $G(t)$ times were shifted (slowed) by a factor of 3.5 in order to mimic the $\Phi(t)$ behavior, which is relevant to dielectric measurements. This factor was found to be virtually independent of temperature and was calculated from the ratio $\tau_{\mathrm{av},\Phi(t)}/\tau_{\mathrm{av},G(t)}$ at temperatures $T = 603$ K and $T = 496$ K where $\Phi(t)$ ACFs are sufficiently relaxed inside the examined time window. The temperature dependence of the predicted $\Phi(t)$ times are in good agreement with the Arrhenius behavior of the β-relaxation. Furthermore, the relative time difference between the DRS β-process and the low temperature NMR methyl motion, is closely reproduced by the difference among simulation times for the methyl process and for $\Phi(t)$ spectra, respectively. In addition, the corresponding average times follow the experimentally observed WLF behavior.

Although there is no direct experimental evidence for the existence of the proposed mechanism, the above results combined with the observations described earlier, are consistent with the conjectured relation between the β-relaxation and the methyl rotation,[37,10] as well as with the relation of these methyl-associated motions to backbone dynamics.

B. Discussion on the Neutron Scattering Results. In the recent NSE and IQENS studies,[11,10] evaluation of the results was based on the dielectrically observed motion. Assuming for the β-process a distribution of relaxation times $g(\ln \tau)$ identical to the one determined by DRS, it was possible to calculate absolute

relaxation times in reasonable agreement with dielectric data. However, a discordance was found in the length scales of the detected motion between NSE and IQENS measurements. Bearing in mind that NSE experiments probe coherent scattering to which a methyl rotation would be invisible, whereas self-motion from methyl hydrogens would strongly contribute to incoherent scattering probed by IQENS, the authors in ref 10 conjectured that the observed discrepancy could be taken as a signature for the involvement of a rotational motion. In view of the relation of the dielectric process with methyl motion, as well as the coupling between the backbone t−t process to methyl dynamics which can survive at sub-T_g temperatures, the differences concerning the underlying mechanism of the β-relaxation as probed by the two neutron techniques, can be qualitatively rationalized: the IQENS experiments may probe β-relaxation mainly through the predominant incoherent scattering of the methyl hydrogen motion, which involves hydrogen displacements larger than 1.78 Å as discussed earlier, while NSE experiments probe it through the coupling between the backbone and the methyl motion, which no longer corresponds to a simple methyl rotation and thus is expected to have nonvanishing coherent scattering amplitude. Taking thus into account that methyl motion at the low-temperature regime cannot be described by a "frozen-backbone"−"mobile-methyl-group" model according to the simulation results, the unsuccessful attempt to fit the IQENS data to a three jump site model[10] becomes comprehensible. The two-site model for EISF, which was found to provide a good description of the β-relaxation, may result from an "effective" geometry of the motion considering the coupling mechanisms present.

To proceed to a quantitative account for the neutron results, simulations at lower temperatures of both coherent and incoherent scattering are required. This issue will be addressed in a future study.

VII. Summary/Conclusions

In the first part of this work, the characterization of the methyl motion in bulk PIB has been addressed by means of molecular dynamics computer simulations and ^{13}C T_1 NMR measurements. Detailed analysis of the temporal and spatial features of methyl motion, combined with a study of the associated conformational statistics, revealed that methyl dynamics in PIB is of composite nature involving strong coupling with backbone motion.

In the high-temperature regime (more than 200 K above the glass transition temperature), a contribution originating from backbone conformational motion in time scales of tens to hundreds of picoseconds (depending on the temperature examined) appears in methyl dynamics, as probed by the reorientation of the methyl C−H bond (the main broad process in $G(t)$, Figure 6) or the displacement of the relevant hydrogen atoms (the intermediate and the slow processes in $S(q,t)$, Figures 2−4). The temperature dependence of the main broad process characterizing $G(t)$ (at $T \geq 388$ K) is in good agreement with the one extracted from the new high-temperature NMR measurements (Figure 8).

In particular, coupling of methyl motion to the trans−trans backbone process is always present, as revealed from the analysis of the coupled transitions. This coupling is expected to persist down to the sub-T_g regime, since the t−t mechanism is a rapid process (faster then methyl jumps) with a very low activation energy. As a result, the methyl rotation, even at low temperatures where it would be decoupled from the practically frozen slow backbone conformational motion, would still be a composite process differing from a simple 3-fold symmetric methyl rotation. The temperature behavior of this process as resolved by the $S(q,t)$ spectra (the intermediate process appearing in the DRTs in Figures 3 and 4) is in close agreement with the extrapolation of the low-temperature NMR data (the so-called δ-process) which has been ascribed to methyl rotation (see Figure 8).

In the second part of this study, the nature of the dielectric β-relaxation observed in PIB and its connection to methyl dynamics was explored. Following indications for the existence of concerted rotation of CH_3 groups attached to the same carbon, as well as other indirect experimental indications mentioned in section VIB, we have examined whether the dynamic behavior of a *combined motion* of these two methyls exhibit the characteristics of the dielectric β-process. It was found that the intermediate process appearing in the respective DRTs showed almost the same temperature dependence and a characteristic time scale close to the high-temperature extrapolation of the dielectric β-relaxation (Figure 12). The time-difference between the new mechanism and the methyl process which was mentioned above, was found to be in a good agreement with the one observed between the dielectric β-relaxation and the NMR δ-process. Furthermore, the average time (including all the observed processes) of this dynamic mechanism followed the experimentally observed WLF temperature behavior.

The coupling between methyl rotation and backbone motion and the suggested mechanism through which they are related to β-relaxation comes as a further step toward a common interpretation of all the available experimental data, as recently proposed.[37] It is clear though that more steps involving both new experiments (e.g., neutron scattering experiments in partially deuterated samples or further low-temperature/high-frequency NMR measurements) and further analysis in combination with new simulations extended to lower temperatures are still required, to shed more light on the mechanisms that are responsible for the peculiar behavior of PIB.

Acknowledgment. Financial support from the TMR network "New routes to understanding polymer materials using experiments and realistic modeling," under Contract ERB-FMRX-CT98-0176 is gratefully acknowledged. The authors wish to thank C. Gaillet for the help in performing the NMR experiments.

References and Notes

(1) Slichter, W. *J. Polym. Sci.: Part C* **1966**, *14*, 133.
(2) Törmälä, P. *J. Macromol. Sci.—Rev. Macromol. Chem. C* **1979**, *17*, 297.
(3) Suter, U.; Saiz, E.; Flory, P. *Macromolecules* **1983**, *16*, 1317.
(4) Dejean de la Batie, R.; Lauprêtre, F.; Monnerie, L. *Macromolecules* **1989**, *22*, 2617.
(5) Vacatello, M.; Yoon, D. *Macromolecules* **1992**, *25*, 2502.
(6) Cho, D.; Neuburger, N.; Mattice, W. *Macromolecules* **1992**, *25*, 322.
(7) Frick, B.; Richter, D. *Phys. Rev. B* **1993**, *47*, 14795.
(8) Bandis, A.; Wen, W.; Jones, E.; Kaskan, P.; Zhu, Y.; Jones, A.; Inglefield, P.; Bendler, J. *J. Polym. Sci.: Polym. Phys. Ed.* **1994**, *32*, 1707.
(9) Rizos, A.; Ngai, K.; Plazek, D. *Polymer* **1997**, *38*, 6103.

(10) Arbe, A.; Colmenero, J.; Frick, B.; Monkenbusch, M.; Richter, D. *Macromolecules* **1998**, *31*, 4926.
(11) Richter, D.; Arbe, A.; Colmenero, J.; Monkenbusch, M.; Farago, B.; Faust, R. *Macromolecules* **1998**, *31*, 1133.
(12) Frick, B.; Alba-Simonesco, C. *Phys. Rev. B* **1999**, *266*, 13.
(13) Karatasos, K.; Saija, F.; Ryckaert, J.-P. *Physica B* **2001**, *301*, 119.
(14) McCrum, N.; Read, B.; Williams, G. *Anelastic and Dielectric Effects in Polymeric Solids*; Wiley: London, 1967.
(15) Karatasos, K.; Ryckaert, J.-P. *Macromolecules* **2001**, *34*, 7232.
(16) Bée, M. *Quasielastic Neutron Scattering;* Adam Hilger: Bristol, England, and Philadelphia, PA, 1988.
(17) Karatasos, K.; Adolf, D.; Hotston, S. *J. Chem. Phys.* **2000**, *112*, 8695.
(18) Narten, A. *J. Chem. Phys.* **1979**, *70*, 299.
(19) Eichinger, B.; Flory, P. *Macromolecules* **1968**, *1*, 285.
(20) Provencher, S. *Comput. Phys. Commun.* **1982**, *27*, 229.
(21) Provencher, S. A general-purpose constrained regularization method for inverting photon correlation data. In *Photon Correlation Techniques in Fluid Mechanics*; Schulz-DuBois, E. O., Ed.; Springer-Verlag: Berlin, 1983.
(22) Gomez, D.; Alegria, A.; Arbe, A.; Colmenero, J. *Macromolecules* **2001**, *34*, 503.
(23) Chahid, A. Alegria, A.; Colmenero, J. *Macromolecules* **1994**, *27*, 3282.
(24) Ediger, M. *Annu. Rev. Phys. Chem.* **2000**, *51*, 99.
(25) Roe, R.; Rigdby, D.; Furuya, H.; Takeuchi, H. *Comput. Polym. Sci.* **1992**, *2*, 32.
(26) Lindsey, C.; Patterson, G. *J. Chem. Phys.* **1980**, *73*, 3348.
(27) van Zon, A.; de Leeuw, S. W. *Phys. Rev. E* **1999**, *60*, 6942.
(28) Mukhopadhyay, R.; Alegria, A.; Colmenero, J. *Macromolecules* **1998**, *31*, 3985.
(29) Moe, N.; Ediger, M. *Macromolecules* **1995**, *28*, 2329.
(30) Alvarez, A.; Arbe, A.; Colmenero, J. *Chem. Phys.* **2000**, *261*, 47.
(31) Frick, B.; Fetters, L. *Macromolecules* **1994**, *27*, 974.
(32) Arrighi, V.; Ferguson, R.; Lechner, R.; Telling, M.; Triolo, A. *Physica B* **2001**, *301*, 35.
(33) Alvarez, F.; Alegria, A.; Colmenero, J.; Nicholson, T.; Davies, G. *Macromolecules* **2000**, *33*, 8077.
(34) Woessner, D. *J. Chem. Phys.* **1962**, *36*, 1.
(35) Boyd, R.; Breitling, S. *Macromolecules* **1972**, *5*, 1.
(36) Karatasos, K.; Anastasiadis, S.; Semenov, A.; Fytas, G.; Pitsikalis, M.; Hadjichristidis, N. *Macromolecules* **1994**, *27*, 3543.
(37) Richter, D.; Monkenbusch, M.; Arbe, A.; Colmenero, J.; Farago, B.; Faust, R. *J. Phys.: Condens Matter* **1999,** *22*, 927.
(38) Londono; et al. *J. Polym. Sci., Part B: Polym. Phys.* **1996**, *34*, 3055.

MA011290M